

Spin simulations in eRHIC Wien filter

F. Meot

September 2019

Collider Accelerator Department
Brookhaven National Laboratory

U.S. Department of Energy

USDOE Office of Science (SC), Nuclear Physics (NP) (SC-26)

Notice: This technical note has been authored by employees of Brookhaven Science Associates, LLC under Contract No. DE-SC0012704 with the U.S. Department of Energy. The publisher by accepting the technical note for publication acknowledges that the United States Government retains a non-exclusive, paid-up, irrevocable, world-wide license to publish or reproduce the published form of this technical note, or allow others to do so, for United States Government purposes.

DISCLAIMER

This report was prepared as an account of work sponsored by an agency of the United States Government. Neither the United States Government nor any agency thereof, nor any of their employees, nor any of their contractors, subcontractors, or their employees, makes any warranty, express or implied, or assumes any legal liability or responsibility for the accuracy, completeness, or any third party's use or the results of such use of any information, apparatus, product, or process disclosed, or represents that its use would not infringe privately owned rights. Reference herein to any specific commercial product, process, or service by trade name, trademark, manufacturer, or otherwise, does not necessarily constitute or imply its endorsement, recommendation, or favoring by the United States Government or any agency thereof or its contractors or subcontractors. The views and opinions of authors expressed herein do not necessarily state or reflect those of the United States Government or any agency thereof.

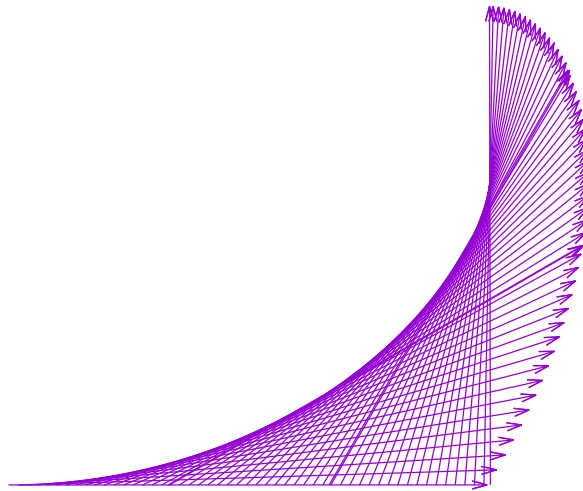
Spin Simulations in eRHIC Wien Filter

François Méot, Erdong Wang
Collider-Accelerator Department, BNL, Upton, NY 11973

September 18, 2019

Abstract

This Tech. Note introduces to a simulation of spin dynamics in a Wien filter used as a spin rotator, based on (i) the use of a semi-analytical model for the electrostatic and magnetostatic vectors and (ii) stepwise ray-tracing techniques. It shows that the method reproduces theoretical expectations.



Contents

1	Introduction	3
2	Theoretical background	3
3	Simulations	3
3.1	Spin motion across the Wien filter	3
3.2	Integration step size	4
3.3	Add fringe fields	5
4	Digressing a little: Pure E	7
4.1	Theory	7
4.2	Simulations	8
5	Launching a bunch through the Wien filter	8

1 Introduction

An option to set the spins vertical prior to injection into eRHIC linac, from longitudinal orientation at the exit of the electron source, is to use a Wien filter. Principles and detailed parameters of the device can be found in eRHIC pCDR [2].

Stepwise ray-tracing techniques can be used to explore properties of spin motion through that $\vec{E} \times \vec{B}$ field. This Tech. Note details the implementation of such simulations, and demonstrates accord with theory.

These exercises are an excerpt from zgoubi workshop tutorials, held in Boulder, Aug. 2019 [1].

2 Theoretical background

Hypotheses: The Wien filter length is L . Take $\vec{E} \parallel \vec{Y}$ and $\vec{B} \parallel \vec{Z}$, with X the main propagation axis, as sketched in Fig. 1.

Take $E_Y = v B_Z$ for a straight electron trajectory.

An expression for the spin rotation may be obtained by analogy between the Lorentz equation and the spin motion equation, namely, from

$$d\vec{v}/ds = \vec{v}' = \vec{v} \times \vec{B}/B\rho \Rightarrow \text{deviation} = BL/B\rho \quad (1)$$

one infers

$$\vec{S}' = \vec{S} \times \vec{\omega}/B\rho \Rightarrow \theta_s = \omega L/B\rho \quad (2)$$

In the present $\vec{E} \times \vec{B}$ configuration, in particular $\vec{B} \perp \vec{v}$ always, one has

$$\vec{\omega} = (1 + a\gamma)\vec{B}_\perp + \gamma(a + \frac{1}{\gamma + 1})\frac{\vec{E} \times \vec{v}}{c^2} \quad (3)$$

Taking \vec{z} unitary vector along Z , accounting in addition for $\vec{E} \perp \vec{v}$,

$$\vec{B} = B_Z \vec{z}, \quad \vec{E} \times \vec{v} = -v E_Y \vec{z} = -v^2 B_Z \vec{z}, \quad \vec{\omega} = \omega \vec{z} \quad (4)$$

With these ingredients ω can be substituted in the θ_s expression above (Eq. 2) to yield

$$\theta_{s.th} = \underbrace{(1 + a\gamma)\frac{B_Z L}{B\rho}}_{=50.588^\circ \text{ from } \vec{B}} - \underbrace{\gamma(a + \frac{1}{\gamma + 1})\beta^2 \frac{B_Z L}{B\rho}}_{=20.588^\circ \text{ from } \vec{E}} = 30^\circ \quad (5)$$

whereas

$$B_Z = \frac{B\rho \theta_{s.th}}{L} / \left[1 + a\gamma - \gamma(a + \frac{1}{\gamma + 1})\beta^2 \right] = 0.0040737834 \text{ T} \quad \text{and} \quad E_Y = v B_Z = 982939.444 \text{ V/m} \quad (6)$$

The numerical values are for one 50 cm segment (of the 3-segment eRHIC Wien filter) which causes a 30° Z-rotation of a 350 keV electron spin.

3 Simulations

WIENFILTER from the code library is used in this exercise (pp. 145 and 264 in [3]). \vec{E} and \vec{B} fields are first taken hard-edge so to allow tight comparison with theory.

3.1 Spin motion across the Wien filter

Approximate magnetic and electric field values are plugged into WIENFILTER, as seen in the input data file (Tab. below, left hand side). A FIT procedure is added to find the convergence of θ_s value to exactly 30° (Tab. below, lower right). The difference in the resulting E, B values compared to the theoretical data (Eq. 6) is negligible (upper right, below).

Fig. 2 shows the rotation of the spin in the \vec{B}^\perp plane along the 3-segment Wien filter.

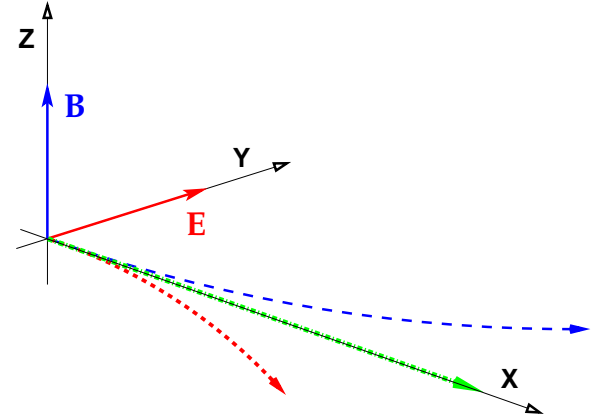


Figure 1: A sketch of the reference frame used and electron motion in pure \vec{E} field (blue) or pure \vec{B} field (red). Under the conjugate effect of both, with proper $E_Y = v B_Z$, the electron trajectory is along the X axis (green) and the spin rotation is 30° over 50 cm path length.

• Input data file (can be copied and executed, as is) with approximate values of E and B (red, blue, respectively) to start the fit procedure (note that E and B signs follow WIENFILTER reference frame conventions):

```
Wien filter used as spin rotator.
'OBJET'
2.3114795386518345 ! Rigidity of a 350 keV electron.
2
3 1 ! 3 electrons, for spin matrix.
0. 0. 0. 0. 0. 1. 'o'
0. 0. 0. 0. 0. 1. 'o'
0. 0. 0. 0. 0. 1. 'o'
1 1 1
'PARTICUL'
0.510998946 1.602176487D-19 1.159652181D-3 0. 0.

'SPNTRK' ! Allows getting the rotation of all 3 spin components
4 ! (they are computed independently), for matrix computation.
1. 0. 0.
0. 1. 0.
0. 0. 1.

'MARKER' #S_WF_tuned ! Needed by 'INCLUDE'
'WIENFILT'
20 ! E and B, approximate
0.5 ! -98.e4 0.004 1 ! E (V/m) and B (T)
0. 0. 0. ! 20. 5. 5. ! Hard-edge entrance face.
0.2401 1.8639 -0.5572 0.3904 0. 0.
0.2401 1.8639 -0.5572 0.3904 0. 0.
0. 0. 0. ! 20. 5. 5. ! Hard-edge exit face.
0.2401 1.8639 -0.5572 0.3904 0. 0.
0.2401 1.8639 -0.5572 0.3904 0. 0.
.1
1. 0. 0. 0.
'MARKER' #E_WF_tuned ! Needed by 'INCLUDE'

'SPNPRT' MATRIX ! spin outcomes, spin rotation matrix.

'FIT2'
2
5 11 0 .1 ! Vary E in WIENFILTER
5 12 0 .1 ! Vary B in WIENFILTER
6 1E-15
3 1 2 #End 0. 1. 0 ! requires straight trajectory.
3 1 3 #End 0. 1. 0 ! id.
10.2 1 1 #End 0.5235987755 1. 0 ! requires 30 deg spin rotation.
10 1 4 #End 1. 1. 0 ! requires |S|=1, for all 3 particles.
10 2 4 #End 1. 1. 0
10 3 4 #End 1. 1. 0

'FAISCEAU' ! Get trajectory coordinates
'SPNPRT' MATRIX ! spin outcomes, including spin rotation matrix.
'END'
```

The optimized E_Y and B_Z values out of the fit, below (red, blue, respectively), yield exact 30° spin rotation: it can be observed that they only differ negligibly from the theoretical values (Eq. 6):

```
*****
STATUS OF VARIABLES (Iteration # 0 / 999 max.)
LMNT VAR PARAM MINIMUM INITIAL FINAL MAXIMUM STEP NAME
5 1 11 -1.081E+06 -9.829E+05 -982939.37 -8.846E+05 8.276E-02 WIENFILT
5 2 12 3.666E-03 4.074E-03 4.07378306E-03 4.481E-03 3.430E-10 WIENFILT

STATUS OF CONSTRAINTS (Target penalty = 1.0000E-15)
TYPE I J LMNT# DESIRED WEIGHT REACHED KI2 NAME
3 1 2 7 0.000000E+00 1.000E+00 3.025031E-10 Infinity SPNPRT
3 1 3 7 0.000000E+00 1.000E+00 1.182248E-08 Infinity SPNPRT
10 1 1 7 5.235988E-01 1.000E+00 5.235988E-01 Infinity SPNPRT
10 1 4 7 1.000000E+00 1.000E+00 1.000000E+00 SPNPRT
10 2 4 7 1.000000E+00 1.000E+00 1.000000E+00 SPNPRT
10 3 4 7 1.000000E+00 1.000E+00 1.000000E+00 SPNPRT
Fit reached penalty value 2.2931E-16

*****
```

Spins, spin matrix (bold) and rotation angle (red), at the end of the Wien filter:

```
*****
10 Keyword, label(s) : SPNPRT MATRIX

INITIAL FINAL
SX SY SZ |S| SX SY SZ |S| GAMMA (Si,Sf) (Z,Sf_X) (Z,Sf)
(Sf_X: projection of Sf & YZ plane) (deg.) (deg.) (deg.)
o 1 1.00000 0.00000 0.00000 1.00000 0.86603 -0.50000 -0.00000 1.00000 1.6849 30.000 -90.000 90.000
o 1 0.00000 1.00000 0.00000 1.00000 0.50000 0.86603 0.00000 1.00000 1.6849 30.000 90.000 90.000
o 1 0.00000 0.00000 1.00000 1.00000 0.00000 -0.00000 1.00000 1.00000 1.6849 0.000 -0.000 0.000

0.866025 0.500000 1.934226E-17
-0.500000 0.866025 -1.508421E-17
-2.429733E-17 3.414397E-18 1.00000

Trace = 2.7320507981, ; spin precession acos((trace-1)/2) = 30.0000005419 deg
Rotation axis : (0.0000, 0.0000, -1.0000) -> angle to (X,Y) plane, angle to X axis: -90.0000, 67.0282 degree
*****
```

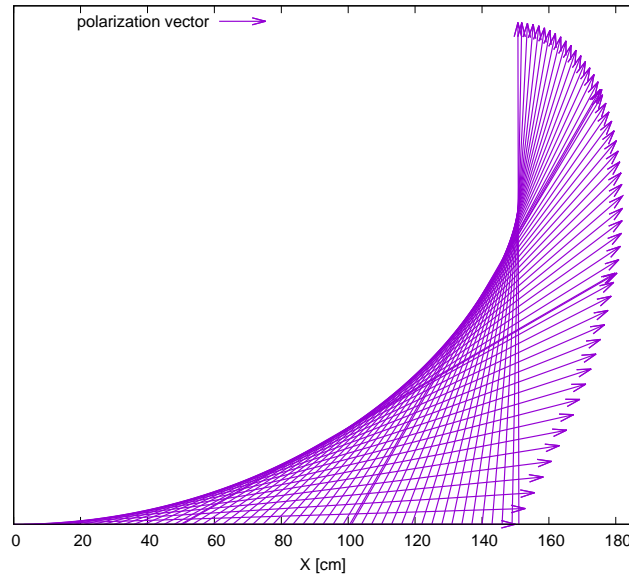


Figure 2: Spin motion in the \vec{B}^\perp plane (the (X,Y) plane in Fig. 1) along the 3-segment Wien filter, from longitudinal at $s=0$ to transverse at $s=151$ cm.

3.2 Integration step size

Numerical convergence of both particle and spin motion may be affected in a non-negligible manner if the integration step size is taken too large. On the other hand the step size should be taken as large as tolerable, if 1000s of particles are to be pushed through WIENFILTER, for statistics purposes for instance.

A scan shown in Fig. 3 indicates that the step size can be several centimeters with minor impact on nominal E or B field amplitudes: these

- Input data file for a step size scan of $\delta E/E$ and $\delta B/B$ (can be copied and executed, as is):

```

Wien filter used as spin rotator.
'OBJET'
2.3114795386518345
2
3 1
0. 0. 0. 0. 0. 1. 'o'
0. 0. 0. 0. 0. 1. 'o'
0. 0. 0. 0. 0. 1. 'o'
1 1 1
'PARTICUL'
0.510998946 1.602176487D-19 1.159652181D-3 0. 0.

'SPNTTRK'
4
1. 0. 0.
0. 1. 0.
0. 0. 1.

'MARKER' #S_WF_tuned
'WIENFILT'
0
0.5 -982939.37 4.07378306E-03 1
0. 0. 0.
0.2401 1.8639 -0.5572 0.3904 0. 0.
0.2401 1.8639 -0.5572 0.3904 0. 0.
0. 0. 0.
0.2401 1.8639 -0.5572 0.3904 0. 0.
0.2401 1.8639 -0.5572 0.3904 0. 0.
.1
1. 0. 0. 0.
'MARKER' #E_WF_tuned

'FIT2'
2 nofinal
5 11 0 1.05
5 12 0 1.05
6 1E-15
3 1 2 #End 0. 1. 0
3 1 3 #End 0. 1. 0
10.2 1 1 #End 0.523598775598299 1. 0
10 1 4 #End 1. 1. 0
10 2 4 #End 1. 1. 0
10 3 4 #End 1. 1. 0

'FAISCEAU'
'SPNPRT' MATRIX PRINT

'REBELOTE'
40 0.1 0 1
1
WIENFILT 80 0.01:10.

'SYSTEM'
2
gnuplot <./gnuplot_scanEB.gnu
okular ./gnuplot_scanEB.eps &
'END'

```

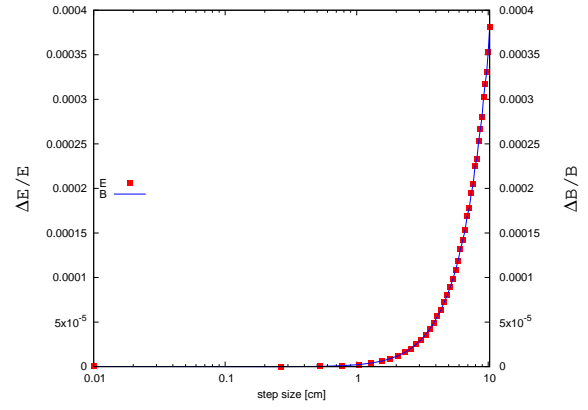


Figure 3: An integration step size scan. This graph shows, as a function of step size, the variation of the E_Y and B_Z fields, relative to their theoretical value, necessary to get (i) exact 30° spin rotation, (ii) straight trajectory.

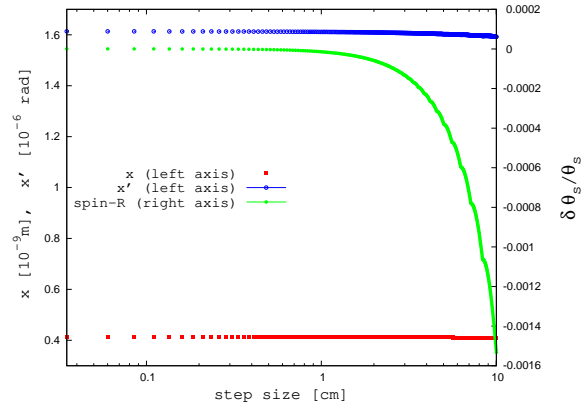


Figure 4: An integration step size scan. This graph shows, as a function of step size, the value of the final position and angle (left vertical axis) and of the relative error on the spin rotation θ_s , compared to 30° , remains below 10^{-3} if the step size remains below 8 cm. Meaning that particles can be pushed through the Wien filter in about 20 steps, extremely quick.

need be tweaked by less than 10^{-3} (relative) compared to their theoretical values to recover 30° spin rotation and straight trajectory. Fig. 4 shows that the adverse effect of a greater step size (on spin rotation and off axis particle deviation) can be compensated by resetting E_Y and B_Z to yield $\theta_s \equiv 30^\circ$.

Conversely, Fig. 4 shows that, for E_Y and B_Z set to their theoretical values, varying the step size has negligible effect on particle position and angle at the exit of the Wien filter segment, whereas the relative error on the spin rotation θ_s , compared to 30° , remains below 10^{-3} if the step size remains below 8 cm. Meaning that particles can be pushed through the Wien filter in about 20 steps, extremely quick.

3.3 Add fringe fields

Adding field fall-offs takes closer to real life, an intermediate stage toward using realistic fields from measured or computed field maps (the latter are available [2, Sec. 2.7.1]).

A specimen field profile as used in the present simulations is shown in Fig. 5. Fig. 6 shows that (i) the numerical integration is essentially converged if the step size is below a few millimeter, (ii) straight trajectory through the Wien filter and exact 30° spin rotation can be recovered (so compensating the lack of accuracy of large step size integration) by adjusting E and B by less than $\approx 10^{-4}$ as long as the step size is less than 2 cm.

This is convenient for statistics: with a 2 cm step size, pushing 10,000 particles through the 3-segment (1.5 m) Wien filter takes about 15 seconds CPU. Note that variable step size is available from the code, indexed on the field gradient, which would decrease the CPU time.

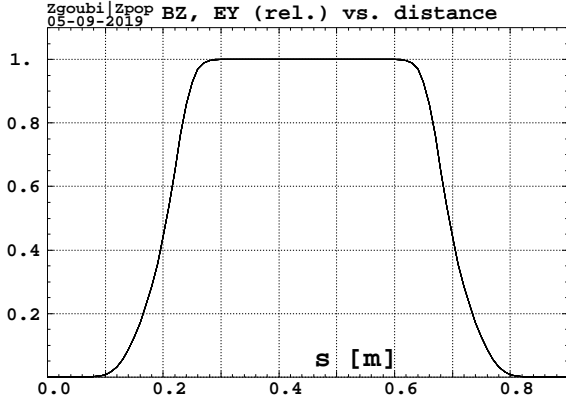


Figure 5: Field shape across a 50 cm Wien filter segment, on-axis, the same for both E_Y and B_Z components here. In the plot of Fig. 7, this fringe field extent is left as is for the E component, while it is varied by $\pm 40\%$ for the B component.

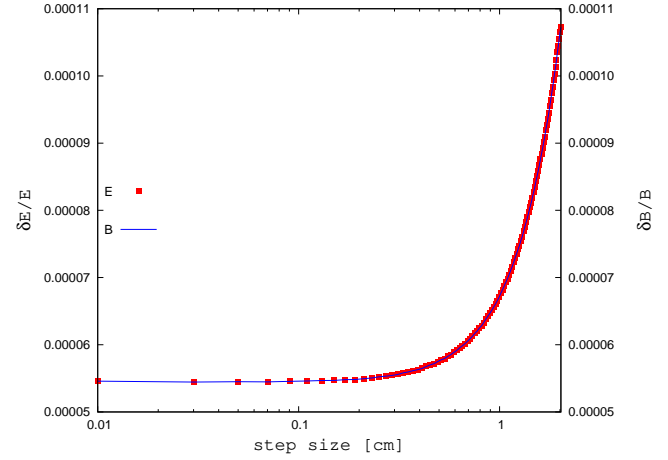


Figure 6: An integration step size scan, including fringe fields. This graph shows that up to 2 cm step size, adjusting the E and B field components by less than 10^{-4} , relative, allows recovering (i) exact 30° spin rotation, (ii) straight trajectory.

Unequal fall off extents - In the case of the OPERA field map of the eRHIC pCDR study, due to a difference in gap [2, Fig. 16, Sec. 2.7.1], the extents of the E and B components are different, and as a consequence the nominal fields of the hard-edge model, and in particular the condition $E_Y = v B_Z$, no longer ensure a straight trajectory.

Fig. 7 shows that, in that case, it is possible (the very low “penalty” value, right vertical axis in the figure), using the two knobs δE_Y and δB_Z , to recover simultaneously a straight trajectory through the Wien filter and exact 30° spin rotation.

- Input data file (can be copied and executed, as is) for a scan of λ_E/λ_B E and B fringe field extent ratio:

```
Wien filter used as spin rotator. A scan of the l_E/l_B fall-off ratio.
'OBJET'
2.3114795386518345      ! Rigidity of a 350 keV electron.
2
3 1
0. 0. 0. 0. 0. 1. 'o'
0. 0. 0. 0. 0. 1. 'o'
0. 0. 0. 0. 0. 1. 'o'
1 1 1
'PARTICUL'
0.510998946 1.602176487D-19 1.159652181D-3 0. 0.
'SPNTNR'      ! Allows checking rotation of all 3 spin components.
4      ! (they are computed independently)
1. 0. 0.
0. 1. 0.
0. 0. 1.
'WIENFILT'
0
0.5 -982939.37 4.07378306E-03 1
20. 5. 5.      ! Hard-edge entrance face. l_E=l_B=5cm
0.2401 1.8639 -0.5572 0.3904 0. 0.
0.2401 1.8639 -0.5572 0.3904 0. 0.
20. 5. 5.      ! Hard-edge exit face. l_E=l_B=5cm
0.2401 1.8639 -0.5572 0.3904 0. 0.
0.2401 1.8639 -0.5572 0.3904 0. 0.
.1
1. 0. 0. 0.
'FIT2'
2 nofinal
4 11 0 1.05      ! vary EY      in attempt to recover straight
4 12 0 1.05      ! vary BZ      trajectory and 30deg spin rotation
6 1E-15 999
3 1 2 #End 0. 1. 0      ! zero orbit position
3 1 3 #End 0. 1. 0      ! zero orbit angle
10.2 1 1 #End 0.523598775598299 1. 0      ! 30deg spin rotation
10 1 4 #End 1. 1. 0
10 2 4 #End 1. 1. 0
10 3 4 #End 1. 1. 0
'REBELOTE'
500 0.1 0 1
1
WIENFILT 22 3.:7.      ! vary l_B from 3 to 7 cm
WIENFILT 52 3.:7.
'END'
```

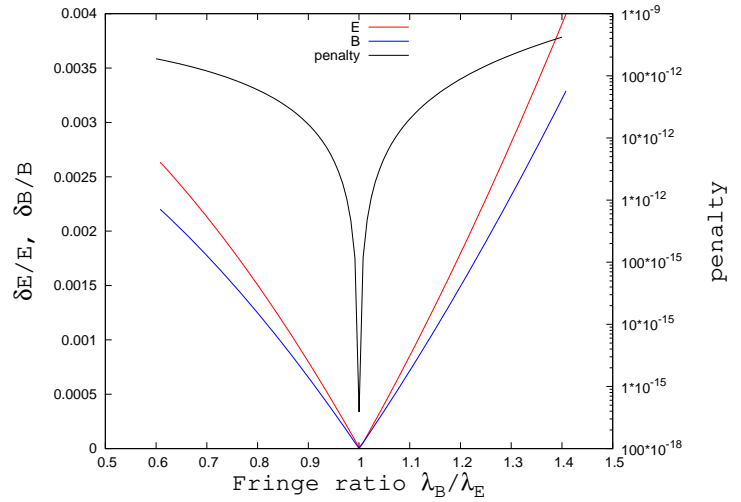


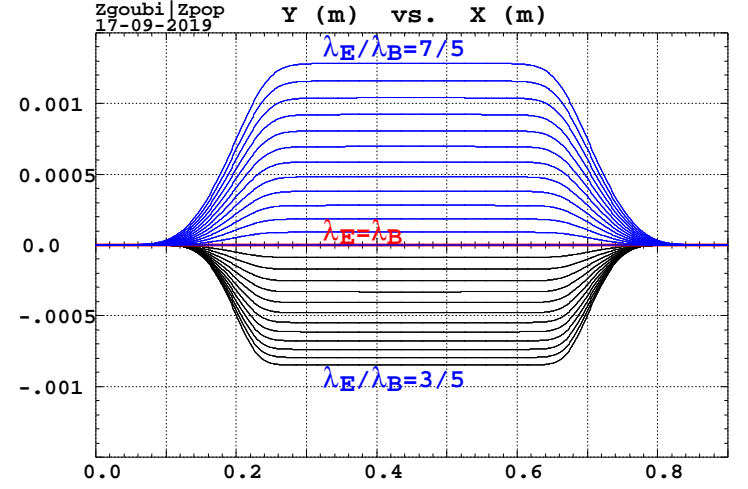
Figure 7: This graph shows the variation of the E_Y and B_Z fields (relative to their hard-edge model values), necessary to recover (i) exact 30° spin rotation, (ii) straight trajectory, when the λ_E/λ_B ratio is varied (B extent varied, while E extent maintained constant in this case). The fit “penalty” quantifies the distance to these two constraints, steadily small here.

As stressed in [2], unequal E and B fall-off extents cause a shift of the orbit inside the Wien filter, this is illustrated below. The orbit is anyway zeroed at the exit (together with maintaining $\theta_s = 30$ deg) by adjusting E and B amplitudes as discussed above (Fig. 7).

- A template input data file for a λ_E/λ_B scan. An external (python) file changes “fringeExtents” to an actual numerical pair ($3 \leq \lambda_E \leq 7$; $\lambda_B = 5$), in 25 iterations here.

```
'OBJET'
2.3114795386518345      ! Rigidity of a 350 keV electron.
2
3 1
0. 0. 0. 0. 0. 1. 'o'
0. 0. 0. 0. 0. 1. 'o'
0. 0. 0. 0. 0. 1. 'o'
1 1 1
'PARTICUL'
0.510998946 1.602176487D-19 1.159652181D-3 0. 0.
'SPNTRK'      ! Allows checking rotation of all 3 spin components.
4      ! (they are computed independently)
1. 0. 0.
0. 1. 0.
0. 0. 1.
'MARKER' #S_WF_tuned
'WIENFILT'
2
0.5 -982939.37 4.07378306E-03 1
20.
fringeExtents
0.2401 1.8639 -0.5572 0.3904 0. 0.
0.2401 1.8639 -0.5572 0.3904 0. 0.
20.
fringeExtents
0.2401 1.8639 -0.5572 0.3904 0. 0.
0.2401 1.8639 -0.5572 0.3904 0. 0.
.1
1. 0. 0. 0.
'MARKER' #E_WF_tuned      ! Needed by 'INCLUDE'
'FIT2'
2 nofinal
5 11 0 .05
5 12 0 .05
6 1E-15 999
3 1 2 #End 0. 1. 0
3 1 3 #End 0. 1. 0
10.2 1 1 #End 0.523598775598299 1. 0
10 1 4 #End 1. 1. 0
10 2 4 #End 1. 1. 0
10 3 4 #End 1. 1. 0

'FAISCEAU'      ! Get some trajectory and some
'SPNPR' MATRIX PRINT ! spin outcomes, including spin rotation matrix.
'END'
```



A scan of the on-momentum orbit across the Wien filter, with varying fringe field extent ratio λ_E/λ_B . The orbit is zero at entrance by hypothesis, and zeroed at the exit (together with maintaining $\theta_s = 30$ deg) by adjusting E and B amplitudes.

4 Digressing a little: Pure E

Here we digress from the Wien filter proper to inspect spin rotation in pure electrostatic field (case of a parallel plate condenser).

The main goal is additional benchmarking against theory, and inspecting ray-tracing accuracy in E fields. The difficulty accuracy-wise, stems from the fact that the rigidity of the particle varies, by contrast to the motion in pure magnetic field.

4.1 Theory

Pure E is obtained by switching off the B_Z component in WIENFILTER. The motion of the particle is in this case a catenary, with equation

$$Y_{th}(X) = \frac{E_i}{eE_Y} \left(\cosh \frac{eE_Y X}{\beta_i E_i} - 1 \right) = \frac{a}{\beta_i} \left(\cosh \frac{X}{a} - 1 \right) \quad (7)$$

with E_i initial total energy, $c\beta_i$ initial velocity, e elementary charge. The length of the catenary from the origin at $(X=0, Y=0)$ to $(X, Y(X))$ is

$$l_{th}(X) = \int_0^X [1 + Y'^2(X)]^{1/2} dX = \int_0^X \left[1 + \left(\frac{1}{\beta_i} \sinh \frac{X}{a} \right)^2 \right]^{1/2} dX = -ia E(i \frac{X}{a}, \beta_i^{-2}) \approx X + \frac{1}{6\beta^2} \frac{X^3}{a^2} + \left(\frac{1}{3} - \frac{1}{4\beta^2} \right) \frac{1}{10\beta^2} \frac{X^5}{a^4} + \dots \quad (8)$$

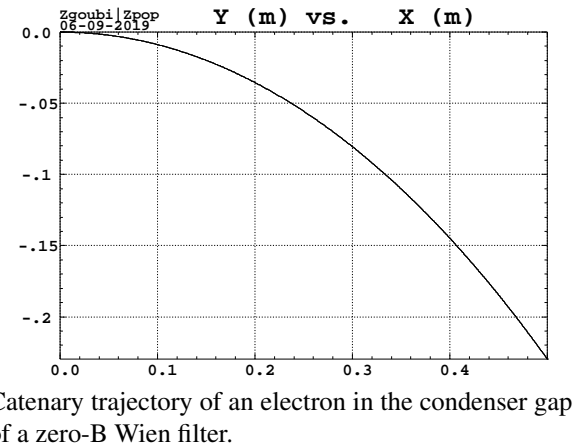
with $E(x, k)$ the elliptic integral of the second kind, i the imaginary unit and, to the right, a series approximation¹. In the present hypotheses, namely

$$E_Y = 982939.4 \text{ V/m (Eq.6)}, \quad E_i = 0.35 + 0.51099894 \text{ MeV} \quad (9)$$

this yields the theoretical values

$$Y_{th}(X = 0.5) = -0.2296924 \text{ m (Eq.7)} \quad \text{and} \quad l_{th} = 0.564150 (\pm 10^{-6}) \text{ m (Eq.8 to } \mathcal{O}(x^{20})) \quad (10)$$

¹Thanks to He Zhao for the Mathematica intervention, BNL, 19-09-10.



Catenary trajectory of an electron in the condenser gap of a zero-B Wien filter.

For the sake of benchmarking, let's assume in a simplified approach that $\vec{E} \perp \vec{v}$, and thus constant energy (it is really not the case, under the effect of \vec{E}). Spin rotation over the distance l across the gap would thus express as (Eqs. 4, 5)

$$\theta_{s.th}|_{\gamma=Const} = \gamma \left(a + \frac{1}{1+\gamma} \right) \frac{\beta E_Y l}{c B \rho} \quad (11)$$

resulting in

$$\theta_{s.th}(l = l_{th})|_{\gamma=Const} = 23.2295425 \text{ deg} \quad (12)$$

Note in passing that this yields $\theta_{s.th}(l = 0.5 \text{ m})|_{\gamma=Const} = 20.58809052 \text{ deg}$, consistent with the contribution from \vec{E} in the $\vec{E} \times \vec{B}$ case, Eq. 5.

4.2 Simulations

Numerical integration is in accord, namely, forcing the electron on-axis (an artifact that stepwise ray-tracing allows) so to force $\gamma = Const$, using a small 0.001 cm step size for greater accuracy, one gets

$$Y(X = 0.5) = -0.2296921 \text{ m}, \quad l = 0.5641488 \text{ m}, \quad \theta_s(l) = 23.2295022 \text{ deg}, \quad \theta_s(0.5 \text{ m}) = 20.5880590 \text{ deg} \quad (13)$$

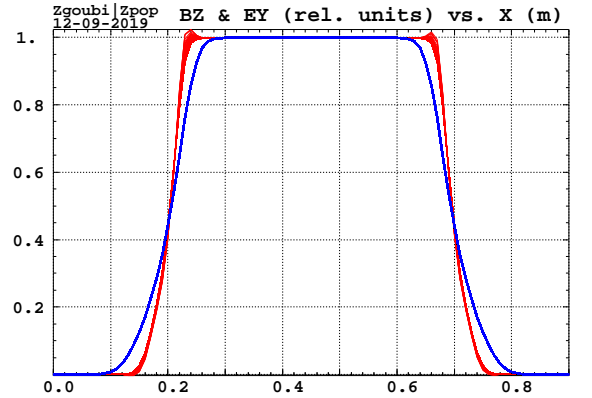
5 Launching a bunch through the Wien filter

A 10^4 particle bunch is considered, *rms* emittances $\beta\gamma\epsilon_Y = \beta\gamma\epsilon_Z = 10\pi\mu\text{m}$, Gaussian transverse densities truncated at 4 sigma, momentum spread uniform in $\pm 10^{-4}$.

The E×B field model of Sec. 3.3 is used here, it includes fringe fields and an exaggerated $\lambda_E/\lambda_B = 3/5$ ratio between E and B fall off extents (figure below). Adjusting the fields at $E_Y = -980189.49$ and $B_Z = 0.00406437546$ ensures straight trajectory and 90° spin rotation, as discussed in Sec. 3.3.

- One third of the spin rotator, as tracked through:

```
'MCOBJET'
2.3114795386518345      ! Rigidity of a 350 keV electron.
3
10000
2 2 2 2 1 1
0. 0. 0. 0. 0. 1.
0. 3.4 7.37e-6 4
0. 3.4 7.37e-6 4
0. 1. 1e-8 2
123456 234567 345678
'PARTICUL'
0.510998946 1.602176487D-19 1.159652181D-3 0. 0.
'SPNTTRK'
4.1      ! Allows choeking rotation of all 3 spin components.
! (they are computed independently)
1. 0. 0.
'WIENFILT'
0
0.5 -980189.49 4.06437546E-03 1
20. 3. 5.
0.2401 1.8639 -0.5572 0.3904 0. 0.
0.2401 1.8639 -0.5572 0.3904 0. 0.
20. 3. 5.
0.2401 1.8639 -0.5572 0.3904 0. 0.
0.2401 1.8639 -0.5572 0.3904 0. 0.
1
1. 0. 0. 0.
'FAISCEAU'
'SPNTPT'
'END'
```



E (red) and B (blue) field (relative units) experienced along sample trajectories across the Wien filter segments. Field fall-off extent scaling factors are $\lambda_E = 3$ and $\lambda_B = 5$, here.

Resulting phase spaces and projected densities, including spin, at the downstream end of the 3-segment Wien filter are shown in Fig. 8.

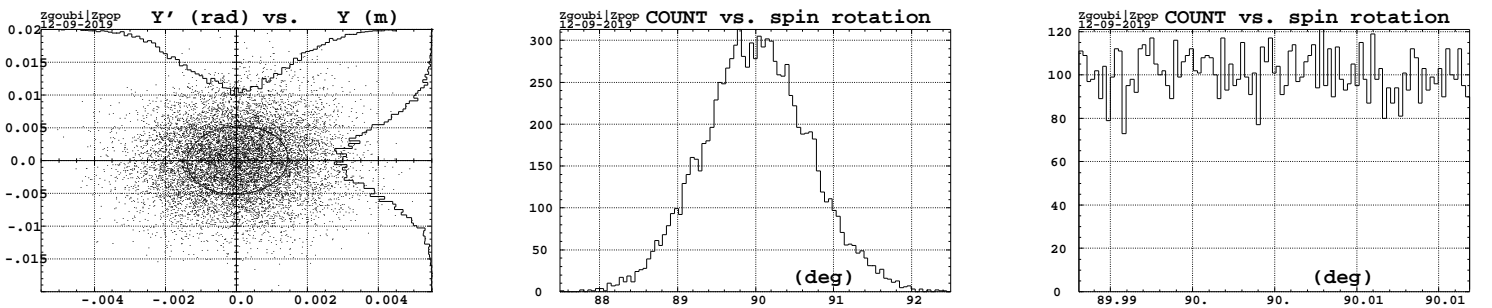


Figure 8: B-normal phase space (left) and spin angle histogram (center) at the exit of the 3-segment Wien filter, case of a 6D bunch with *rms* emittances $\beta\gamma\epsilon_Y = \beta\gamma\epsilon_Z = 10\pi\mu\text{m}$, Gaussian transverse densities truncated at 4 sigma, momentum spread uniform in $\pm 10^{-4}$. The spin angle spreading stems from the B-normal transverse emittance. The right histogram corroborates that: spin angle spreading under the effect of 10^{-4} momentum spread, and with $\epsilon_Y = \epsilon_Z = 0$, amounts to $\approx \pm 0.01 \text{ deg}$

References

- [1] <https://zgoubi-workshop.com/>.
- [2] eRHIC p-CDR, BNL (2018).
- [3] Zgoubi Users' Guide, <https://www.osti.gov/scitech/biblio/1062013-zgoubi-users-guide>.